Fluidized Bed Drying of Solids

A kinetic model is developed for the drying of solids in fluidized beds, assuming a falling rate period following a constant rate period. Experimental data obtained using batch and continuous single and spiral fluidized beds are satisfactorily matched with the assumed drying kinetics and the residence time distribution of solids appropriate for the type of dryer.

A. N. Chandran
S. Subba Rao
Y. B. G. Varma
Department of Chemical Engineering
Indian Institute of Technology
Madras 600 036, India

Introduction

Small particle drying is of importance industrially in the drying of raw materials, intermediates and finished products. Depending on the particle size and the nature of feed, the preferred mode of drying is either spray drying (particle size: 10 to 500 μm), flash drying (10 to 3,000 μm), or fluidized drying (50 to 5,000 μm). While the spray dryers and flash dryers are capable of taking liquid feed, fluidized beds are generally operated with wet solid feed.

Fluidized drying among others has the advantage of high intensity of drying and high thermal efficiency with uniform and closely controllable temperature in the bed. It requires less drying time due to high rates of heat and mass transfer and provides for a wide choice in the drying time of the material. The technique offers ease in operation and maintenance of the dryer, adaptability to automation and for combining several processes such as mixing, classification, drying, and cooling. The disadvantages, on the other hand, include high-pressure drop, attrition of the solids and erosion of the containing surfaces, and a possibility of nonuniform moisture content in the product as a result of the distribution of the residence times of the individual particles.

Fluidized drying of solids can be batchwise or continuous. Batch operation is preferred for small-scale production and for heat-sensitive materials. The process conditions are easily selected in batch drying, and the product is of uniform quality due to homogeneity of the bed at any instant during its operation. In continuous fluidized drying, the product from the dryer under steady-state operation corresponds in its properties to the material within the dryer due to high degree of solids mixing. The residence times of individual particles differ widely within the dryer; hence, the product contains particles dried to different extent. To overcome the drawback, internal baffles are often provided in industrial fluidized dryers of circular cross-section (Jobes, 1954; Frolov et al., 1964) and of rectangular cross-section (Beran and Lutcha, 1975; Reay, 1978).

The mixing character of the solids and the drying kinetics are important in estimating the performance of continuous fluidized dryers. The solids mixing may be approximated to ideal mixing in cylindrical fluidized beds (Vanecek et al., 1966) and to a finite axial Peclet number in rectangular fluidized beds (Beran and Lutcha, 1975). Beran and Lutcha (1975) studied the drying of crystalline ammonium sulfate, assuming a constant rate period preceding the falling rate period for the drying kinetics. Suzuki et al. (1980), however, postulated the drying kinetics to comprise constant rate period followed by first falling rate period and a second falling rate period. Their experimental data obtained using vibratory fluidized beds, however, indicate that a single falling rate period following the constant rate period would suffice to describe the drying kinetics.

A model is developed in the present study for the drying kinetics of solid particles. Experimental data, obtained on drying of solids in batch and continuous fluidized beds, are matched with the predictions based on the model and the appropriate residence time density function describing the mixing of solids.

Model Development

Drying kinetics for batch operation

The following assumptions are made in the development of the drying kinetics for batch drying:

1. The drying rate curve has either constant rate period and/or falling rate period.
2. The falling rate period is linear and is represented by a single line from the critical moisture content to the equilibrium moisture content.
3. The feed conditions of the heating medium remain unaltered during the drying process.
4. The contact area between the solids and the drying medium remains constant for the chosen gas-solid system and conditions.

The equations governing the kinetics of the drying process

Correspondence concerning this paper should be addressed to Y. B. G. Varma.

may be represented as:

Constant Rate Period

$$t = (C_o - C)/R$$

or

$$C = C_o - Rt;\ C \geq C_c;\ t \leq t_c \tag{1}$$

Falling Rate Period

$$t = [(C_c - C^+)/R] \ln [(C_c - C^+)/(C - C^+)]$$

or

$$C = C^+ + (C_c - C^+) \exp [-\beta(t - t_c)];$$
$$C \leq C_c;\ t \geq t_c \tag{2}$$

where β $(=R/[C_c - C^+])$ is the slope of the line representing the falling rate period. R is the drying rate coefficient, expressed as weight of water evaporated per unit weight of dry material and unit time. C_o, C_c, and C^+ represent the initial, critical and equilibrium moisture contents, respectively. The moisture content of the product for a given time in batch drying is estimated using Eqs. 1 and 2 from a knowledge of C_o, C_c, C^+, and R.

Continuous drying of solids

The drying process is different in batch drying from that in continuous drying. In the former, the entire bed is homogeneous at any instant during the process; hence, there is little interaction between the particles as far as drying is concerned. The drying kinetics would suffice here to estimate the time required to effect a given reduction in the moisture content of the solids. In contrast, in continuous operation using single fluidized beds, the particles leaving the bed have a distribution in residence times, necessitating to consider their residence times simultaneous to the drying kinetics. Secondly, at any instant during the process, the bed consists of a small fraction of wet particles (the feed) dispersed in a bed of almost dry particles. This suggests an interaction between the particles. However, the mass and energy transfer between the particles are due primarily to diffusion on collision between the particles, and the thermal constriction resistance depends on the size of contact spots between the particles.

In a fluidized bed, though the number of contacts are large, the time of contact and the area of each contact are less, making the contribution for heat and mass transfer between particles from their interaction considerably smaller when compared to that the particles derive from their contact with the fluid medium. One may assume the fluidizing gas in the continuous fluidized bed to be an infinite source. In the batch operation, the incoming air approaches solid temperature quickly, while the solids approach air temperature almost instantaneously in the continuous operation.

The average moisture content in the product from continuous drying of solids with a distribution in the residence times for the particles may be written as

$$\frac{\bar{C}}{C_o} = \int_o^\infty \left(\frac{C}{C_o}\right)_b E(\theta)\, d\theta \tag{3}$$

where $(C/C_o)_b$ denotes the moisture content in the product relative to the initial moisture content under batch operation. $E(\theta)$ is the residence time density function for the solids, appropriate to the mixing character within the bed.

Single-Stage Fluidized Bed. Assuming ideal mixing for the solids (Vanecek et al., 1970), i.e., $E(\theta) = \exp(-\theta)$, the average moisture content in the product is given by Eqs. 1, 2 and 3 (see Appendix for details of derivation):

$$\frac{\bar{C}}{C_o} = 1 - \frac{R\bar{t}}{C_o} + \exp(-\theta_c) \cdot \left[\frac{R\bar{t}\,\theta_c}{C_o} + \frac{R\bar{t}}{C_o} - \left(1 - \frac{C^+}{C_o}\right) + \left(\frac{C_c - C^+}{C_o}\right)\frac{1}{\beta\bar{t} + 1}\right] \tag{4}$$

On the assumption that the moisture content and the drying rate at the end of the constant rate period are identical to those at the beginning of the falling rate period, Eq. 4 reduces to

$$\frac{\bar{C}}{C_o} = 1 + \frac{R\bar{t}}{C_o}\left[\frac{\beta\bar{t}\exp(-\theta_c)}{\beta\bar{t} + 1} - 1\right] \tag{5}$$

Spiral Fluidized Bed. Pydisetty et al. (1989) developed a spiral fluidized bed, wherein a vertical baffle was provided as spiral over the distributor plate of a single-stage fluidized bed of circular cross-section. Such a bed may be viewed as a long rectangular fluidized bed, wound as a spiral to circular cross-section. The solids, fed continuously to the center of the fluidized bed, move spirally between the leaves of the spiral baffle in fluidized state and discharge through the downcomer provided at the periphery of the fluidized bed. Pydisetty et al. (1989) studied the residence time distribution of solids in spiral fluidized beds and reported that the semiinfinite axial dispersion model given below adequately represented the solids mixing within the bed:

$$E(\theta) = \sqrt{\frac{-Pe}{4\pi}}\,\frac{1}{\theta^{3/2}} \exp\left[-\frac{(1 - \theta)^2\, Pe}{4\theta}\right] \tag{6}$$

The authors related the dispersion number to the system variables as

$$\frac{D_e}{u_s d} = 440\left(\frac{u}{u_s}\right)^{0.3}\left(\frac{h}{d}\right)^{0.1} Fr^{0.7}\, Ar^{-0.7} \tag{6a}$$

Since the solids at any cross-section along the spiral are at uniform moisture content, interparticle collisions do not affect the drying rate of the particles.

On substitution of Eq. 6 in Eq. 3 and solving (see Appendix), one obtains,

$$\frac{\bar{C}}{C_o} = \frac{1}{2} e^{Pe/2}\Big\{e^{Pe/2}(\alpha_1 + \alpha_2)[1 - \operatorname{erf}(k + k\theta_c)] - e^{-Pe/2}(\alpha_1 - \alpha_2)[\operatorname{erf}(k - k\theta_c)] + e^{-Pe/2}[2 - (\alpha_1 + \alpha_2)] + \frac{R}{\beta C_o} e^{\beta\theta_c\bar{t}}\{e^{\gamma\sqrt{Pe}}[\operatorname{erf}(k + \gamma\sqrt{\theta_c}) - 1] + e^{-\gamma\sqrt{Pe}}[\operatorname{erf}(k - \gamma\sqrt{\theta_c}) + 1]\}\Big\} \tag{7}$$

where

$$\alpha_1 = \frac{Rt_c}{C_o} + \frac{R}{\beta C_o}$$

$$\alpha_2 = \frac{R\bar{t}}{C_o}$$

$$k = \sqrt{Pe/4\,\theta_c}$$

$$\gamma = \sqrt{(Pe/4) + \beta\bar{t}}$$

Recognizing that the axial dispersion model describes solids mixing satisfactorily in rectangular fluidized beds, Eq. 7 is also valid to estimate the moisture content of the product from a rectangular fluidized-bed dryer.

Figure 1 shows the variation in the average moisture content of the solids with drying time and the axial dispersion within the bed. It is seen that the average moisture content of the product decreases with an increase in solids-holding time. An increase in the Peclet number for a given solids-holding time increases the bed efficiency due to an approach to piston flow and results in a reduction in the moisture content of the product. This, however, is true only when the drying process corresponds to the falling rate period. During the constant rate period, the kinetics is of zero order in moisture concentration; hence, the mixing has no influence on the drying rate.

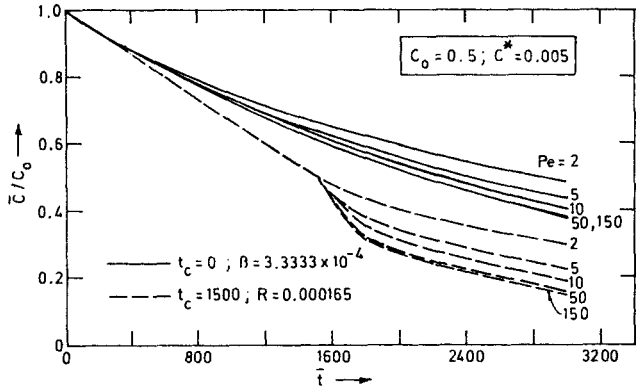

Figure 1. Variation of relative moisture of solids with the mean holding time and the axial Peclet number in the spiral fluidized bed.

Experimental Studies

Figure 2 shows the schematic diagram of the experimental setup and its details. Two fluidization columns of stainless steel were used for the study. Column I was of 398 mm in ID and 470 mm in height, and Column II was of 310 mm in ID and 310 mm in height. The air chamber (8) for Column I consisted of a stainless steel tank of 600 × 600 × 400 mm connected to the air inlet pipe (5) following the heater (4), while for Column II it consisted of a cylindrical stainless steel tank (6) of identical dimen-

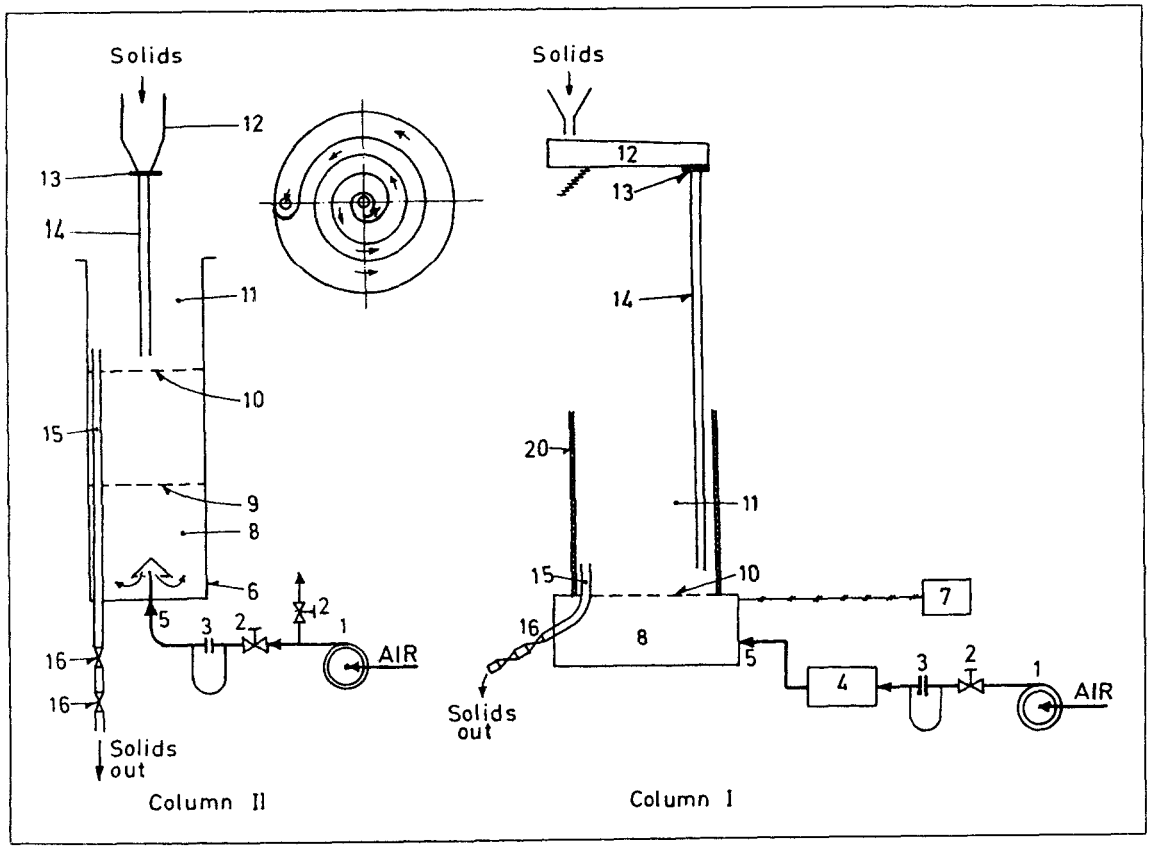

Figure 2. Experimental setup.

1 = blower
2 = control valves
3 = flowmeter
4 = heating section
5 = air inlet
6 = stainless steel tank
7 = temperature controller
8 = air chamber
9 = perforated grid
10 = distributor plate
11 = fluidization section
12 = solids feeder/hopper
13 = calibrated orifice
14 = downflow pipe
15 = downcomer
16 = quick-closing valves

Table 1. Experimental Variables in the Present Study*

Sl No.	Variables	Batch Fluidized Bed	Continuous Fluidized Bed	
			Single Stage	Sprial
1	Column Dia., D, mm	310 and 398	310 and 398	310 and 398
2	Air Flow Rate, Q, m^3/s	0.069 to 0.172	0.092 to 0.152	0.092 to 0.152
3	Inlet Air Temp., T, K	300 to 370	300 to 350	300 to 350
4	Particle Size, d, mm	$-0.5 + 0.315$ to $-1.0 + 0.8$	$-0.8 + 0.5$ to $-1.0 + 0.8$	$-0.8 + 0.5$ to $-1.0 + 0.8$
5	Fluidized Bed Hght., h, mm	40 to 120	55 to 80	55 to 80
6	Solids Flow Rate, G_s, $kg/m^2 \cdot s$	—	0.006 to 0.817	0.011 to 0.817
7	Mean Holding Time, t, s	6,300 (Max)	70 to 2,390	100 to 2,360
8	Channel Length, L, mm	—	—	1,670 to 3,580
9	Channel Width, B, mm	—	—	25.4 to 70

*Material and density: ion-exchange resin (ρ_s = 1,480 kg/m^3); s and (ρ_s = 2,650 kg/m^3).

sions as that used for fluidization column. The air chamber served for uniform distribution of air before it entered the fluidization section. Column II was operated at ambient temperature.

The distributor plate (10) for both of the columns consisted of 2-mm-thick stainless steel sheet with 2-mm perforations to give 13% free area. A fine stainless steel mesh of 0.2 mm was placed over the perforated plate and spot-welded to arrest possible solids leakage through the distributor plate.

The air heater (4) had provision for 8, 12 and 20 kW. The temperature controller (7) had Iron-Constantan thermocouples for a maximum temperature of 150°C with an accuracy of ±0.5°C.

The solids were admitted into the fluidization column in (single-stage) continuous fluidized bed through a downflow pipe (14) located on the column periphery from a hopper/vibratory feeder (12). The flow of solids was controlled using a horizontal calibrated orifice (13) that could laterally slide into the bottom of the hopper. The solids discharged through a 12.5-mm-ID downcomer (15) adjustable for its height to secure different bed heights in the fluidization column. An extended tube, provided on the downcomer with two quick-closing valves (16), prevented the leakage of air.

With spiral fluidized beds, a 350-mm-high, 0.5-mm-thick brass sheet was carefully soldered to the stainless steel mesh of the distributor plate in the form of a spiral. The channel width (clearance between any two leaves of the spiral) was maintained constant, as far as possible. Solids were fed normally at the center of the column and were discharged at the column periphery (Shown in Figure 2 typically for Column II).

Drying Experiments were conducted in batch, continuous single-stage, spiral fluidized beds with the ion-exchange resin (INDION-225) with density of 1,480 kg/m^3 and the sand with density of 2,650 kg/m^3 at different experimental conditions. To prepare the feed of a given moisture content, a definite quantity of water was added to a known amount of solids, mixed thoroughly, and a sample was taken for analysis. The moisture content in the sample was analyzed by keeping it in an air oven maintained at 105°C until constant weight and noting the difference in weight as the amount of water present in the sample. The moisture content of the material was expressed on dry basis.

Air was admitted into the column at the desired rate with the heater switched on until a preset steady-state temperature was attained. In batch drying, a known amount of solids, having known initial moisture content, was fed to the fluidization column. As fluidization continued, solid samples were taken out of the fluidized bed at different clock times and were analyzed for their moisture content.

In continuous fluidized drying of solids, air at the desired rate was admitted into the column at controlled temperature, and the solids of known initial moisture content were fed into the fluidized bed at the desired rate with the product simultaneously removed from the fluidized bed through the downcomer (15). The experiment was continued until the solids inflow rate matched the outflow and, more significantly, until the average moisture content of the discharging solids assumed a steady value. In general, a time of approximately five times the mean holding time of the solids was required to attain the steady state. A sample of the solid from the discharge downcomer was then collected and analyzed for its moisture content. The holdup of the solids was measured by emptying the column after the experiment and weighing its contents accurately.

The experiments of the present study in batch, continuous, single-stage, spiral fluidized beds cover different initial moisture contents of the solids, the particle size, the type of the solids, the flow rates of the phases, the temperature of the heating medium, and the mean residence time of the solids (solids holdup). Table 1 gives the details of the experiment and range of variables covered in the study.

Results and Discussion

Batch fluidized drying of solids

Figure 3 shows typical experimental data on batch fluidized drying of solids for a change in:

- Temperature
- Flow rate of the drying medium
- Initial moisture content of solids
- Particle size
- Holdup (or bed height) of the solids

It is seen from the figures that the batch drying of solids exhibits constant rate period and a falling rate period, whose relative magnitudes depend on the system conditions. The drying rate in the constant rate period is enhanced with an increase in temperature (Figure 3a) and flow rate (Figure 3b) of the heating medium, and is reduced with an increase in the particle size (Figure 3d) and solids holdup (Figure 3e). The presence of constant rate period indicates whether the controlling resistance is limited to external diffusion or to the diffusion of moisture through a layer of crest at the surface. Temperature influences

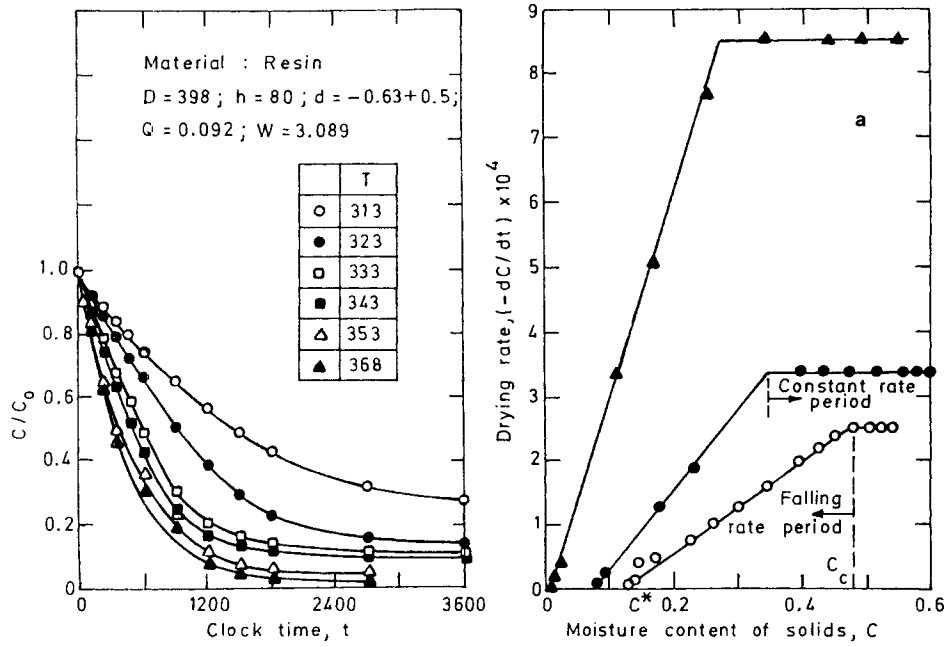

Figure 3a. Relative moisture content of solids with system variables: effect of drying temperature.

little in a diffusion-controlled process, while its effect is slightly higher when external diffusion controls.

The rate of drying is affected by the superficial velocity of the drying medium only when external diffusion is controlling, while the particle size affects the rate of drying when both external and internal diffusion control; its effect, however, is small when the former controls the process. Though the drying rate in the constant rate period is estimated with reasonable accuracy, the prediction of the range of moisture content, over which the constant rate period prevails, is difficult. This range depends on the rate at which moisture is supplied to the surface *vis-a-vis* its evaporation from the surface. The mechanism of this supply may be one of several; but, irrespective of the transfer mechanism, the critical moisture content depends on the heating medium conditions, the properties of the material being dried, and the holdup of the solids. It is observed that the critical moisture content decreases with an increase in the temperature of the heating medium, but increases with an increase in its flow rate. It is further noted that, for an increase in constant drying rate (effected due to an increase in the flow rate of the heating medium), the critical moisture content is higher with an increase in the bed height. These observations are in qualitative agreement with some of those reported in literature in batch drying of solids (Lykow, 1955).

Figure 3 shows that the constant rate period is significantly affected by the temperature and flow rate of the heating

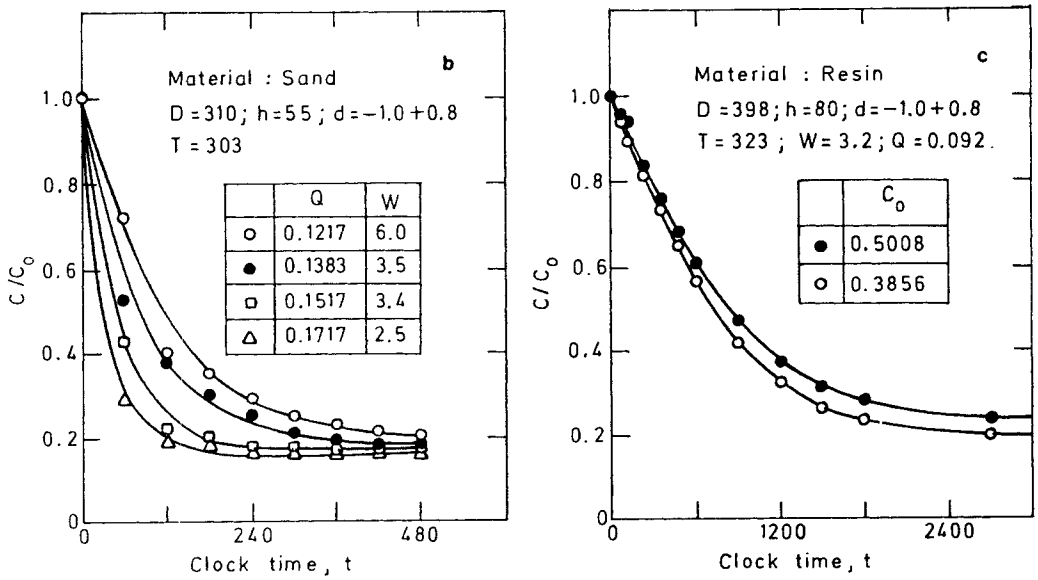

Figure 3b. Relative moisture content of solids with system variables: effect of flow rate of air.

Figure 3c. Relative moisture content of solids with system variables: effect of initial moisture of solid.

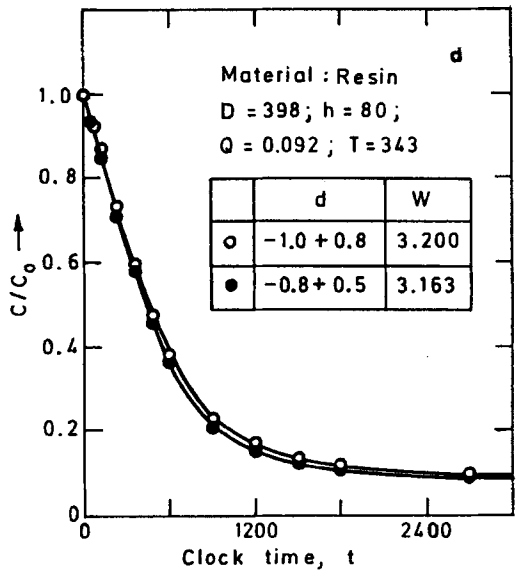

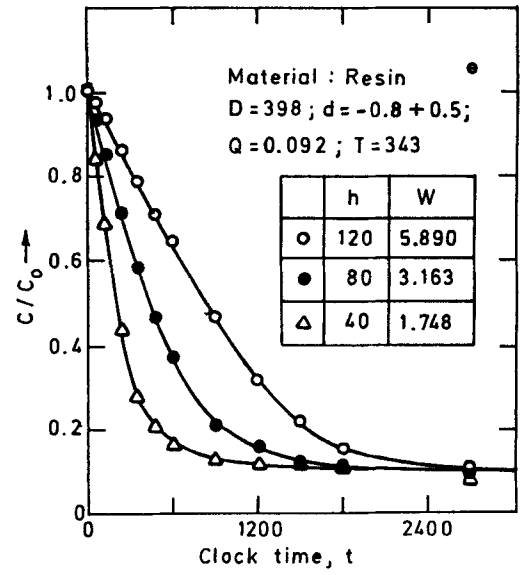

Figure 3d. Relative moisture content of solids with system variables: effect of particle size.

Figure 3e. Relative moisture content of solids with system variables: effect of bed height.

medium, as compared to their effect on the falling rate period. This is expected in view of the fact that the equilibrium moisture content, as compared to the critical moisture content, is a weak function of system variables.

Based on the dependency exhibited by the constant drying rate, the critical moisture content, and the equilibrium moisture content on the system variables, the following emperical relationships are obtained:

$$\left(\frac{RW}{\rho Q}\right) = k_1 \left(\frac{u^2}{gd}\right)^{0.6} \left(\frac{d}{h}\right)^{0.2} \exp\left(\frac{-4{,}000}{T}\right) \tag{8}$$

$$C_c = k_2 (\rho Q)^{-0.03} W^{-0.12} d^{-0.18} C_o^{0.35} \exp\left[\frac{-1{,}000}{T}\right] \tag{9}$$

$$\left[1 - \frac{C^+}{C_o}\right] = k_3 (\rho Q)^{0.04} d^{-0.33} C_o^{-0.26} \exp\left[\frac{1{,}500}{T}\right] \tag{10}$$

The constants, k_1, k_2 and k_3 are 400, 2.1, and 5.72 for ion-exchange resin, and are 24.2, 0.15, and 1.2×10^{-4} for sand, respectively. The energy for activation of 8,000 cal/gmol, given in Eq. 8 for the drying rate coefficient, R is in accordance with that reported by Vanecek et al. (1966) for the diffusion-controlled process. Though the emperical equations given above are specific to the materials and the range of variables covered in the study, the purpose of presenting them is to facilitate the prediction of R, C_c, and C^+, and thus the batch drying rate curve at experimental conditions not significantly different from the range covered in the study. This is to facilitate a comparison of the performance of the batch and continuous fluidized-bed dryers.

For a given choice of the operating conditions, R, C_c, and C^+ are estimated using Eqs. 8 to 10; the parameters are then inserted into the rate equations (Eqs. 1 and 2) to predict the moisture content of the solid. Figure 4a presents typical experimental data and the model, and Figure 4b compares the experimental and predicted moisture content for the batch fluidized drying of resin and sand under different experimental conditions. The satisfactory comparison validates the assumed drying kinetics of a constant rate period followed by a single falling rate period for drying of solids in fluidized beds.

Continuous drying of solids in single-stage fluidized bed

In addition to the variables listed for batch fluidized drying, the effect of solids flow rate on drying rate is investigated in continuous single-stage fluidized bed. The effect of the variables on the drying rate in continuous fluidized bed is qualitatively similar to that reported for batch fluidized drying of solids. The effect of solids flow rate on the drying rate is reflected in its effect on the mean holding time of the solids. An increase in solids flow rate increases the solids holdup, but decreases rapidly the mean holding time of the solids.

Comparing the performance of the continuous fluidized dryer with that of the batch fluidized dryer, it is seen from Figure 5 that for a given drying time, batch operation gives lower average moisture content in the product than the continuous operation. This is in agreement with the observation due to Vanecek et al. (1970) for single cylindrical fluidized bed dryer and due to Beran and Lutcha (1975) for rectangular fluidized-bed dryer.

Romankov (1971), however, reported improved performance under mixed-flow conditions as compared to batch drying. The anamoly may be attributed to the use of pulse input of wet solids into the bed by the author (1971).

Figure 6 compares the experimental data with the prediction using Eq. 5 assuming ideal mixing for solids and drying kinetics as given by Eqs. 1 and 2. The satisfactory comparison between the model and the experiment validates the aforementioned assumptions. For comparison, the experimental data obtained using the batch fluidized bed is also shown in the figure. The difference in the average moisture content of the product between the batch and continuous operation is large, for a given drying time, in the falling rate period, and this difference

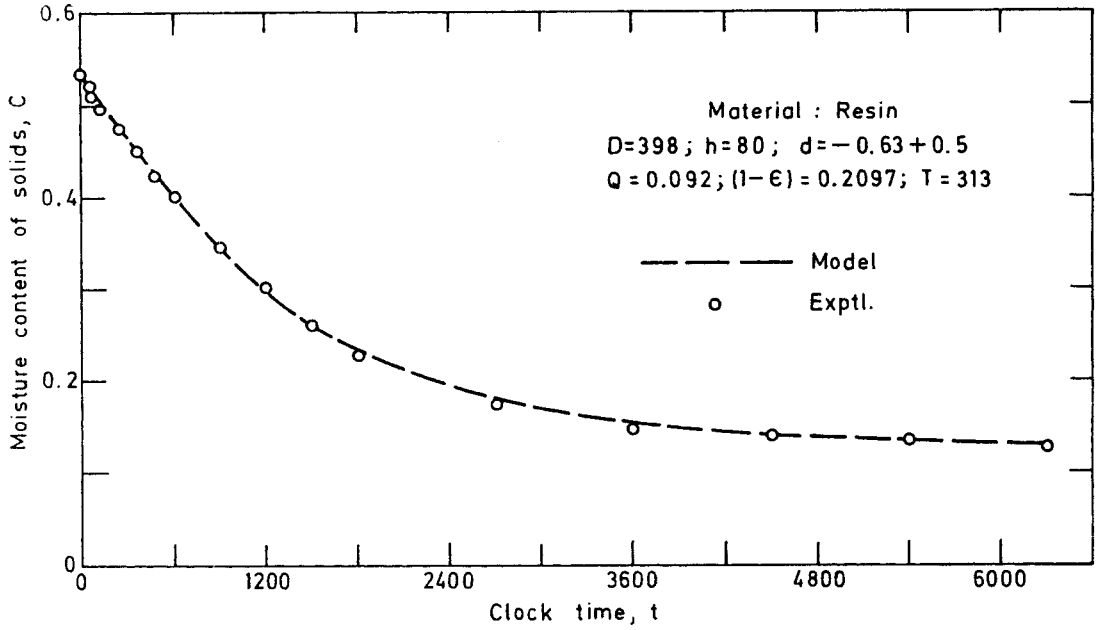

Figure 4a. Experimental data vs. kinetic model for drying of solids in a fluidized bed.

increases as the moisture content approaches the equilibrium moisture content.

Continuous drying of solids in spiral fluidized bed

The effect of the variables such as the temperature of the heating medium, the flow rates of the phases, the particle size, and the solids holdup on the drying of solids in continuous spiral fluidized bed is qualitatively similar to that reported for continuous single-stage fluidized bed. Additionally, the channel length was chosen as one of the variables for investigation, and it is noted that an increase in the channel length for a given diameter of the fluidization column increases the holding time of the sol-

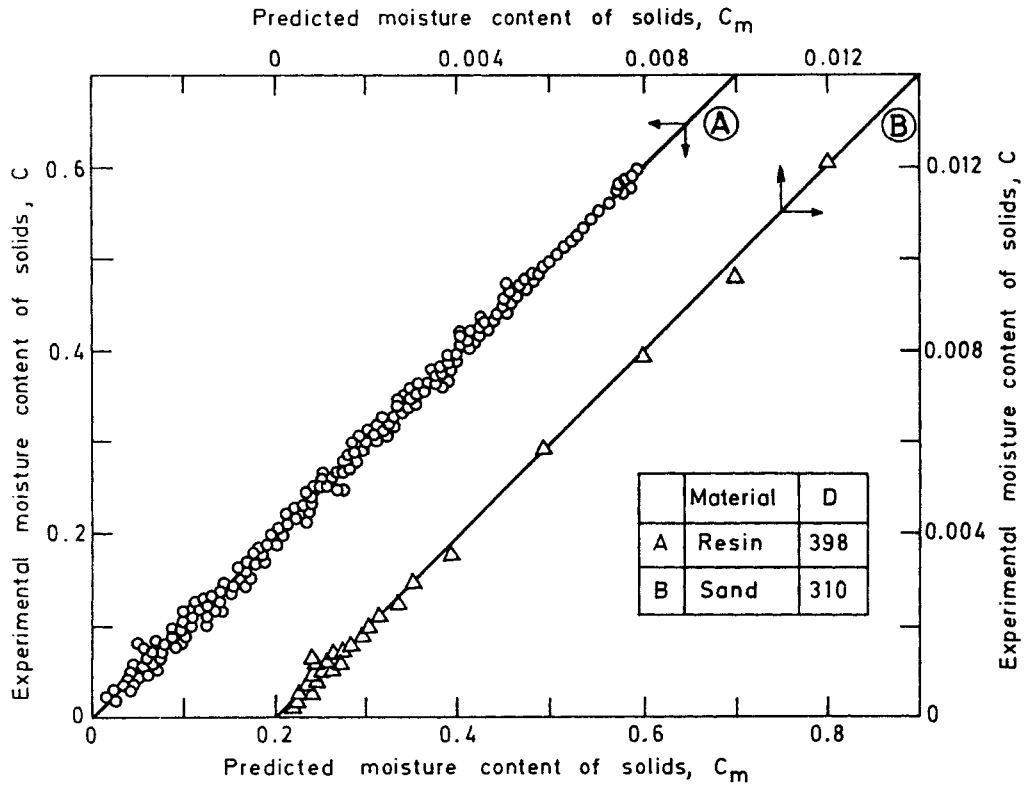

Figure 4b. Predicted vs. experimental moisture content of the solids.
A = ion exchange resin; *B* = sand

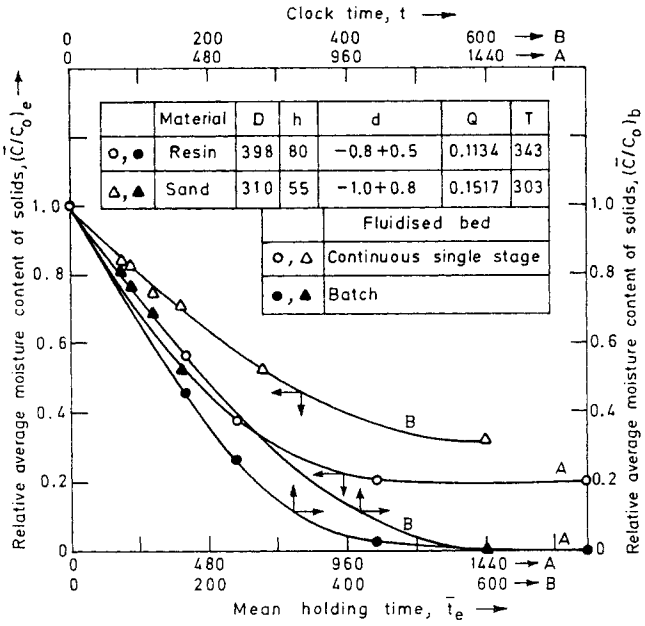

Figure 5. Performance of fluidized-bed dryers: batch vs. continuous.

ids and thus reduces the average moisture content of the product.

Figure 7 compares the experimental data obtained in the spiral fluidized dryer with that predicted using Eq. 7. The satisfactory comparison of the model with the experimental data justifies the use of diffusional mixing model for describing the flow of solids in spiral fluidized bed, as well as the prediction of the dryer performance using Eq. 3. The average moisture content of the product from the spiral fluidized dryer closely corresponds to that from the batch fluidized dryer during the constant rate and falling rate periods, which is attributed to low axial mixing in the spiral fluidized bed.

The performance of the spiral fluidized dryer is, in fact, intermediate to that of single, continuous fluidized bed and the batch fluidized bed dryers (Figure 8). With an increase in axial mixing, it may be expected that the performance of the spiral fluidized-bed dryer approaches that of single fluidized-bed dryer while low axial mixing makes it correspond to that of batch operation. Considering the advantages associated with that of the continuous operation over batch operation, it is evident from figure 8 that the provision of spiral in the single fluidized dryer and operating the same as a spiral fluidized dryer is advantageous.

Summary

The present study on drying of solids in fluidized beds is based on combining the drying kinetics and the residence time density function appropriate for the mixing of solids in the bed to predict the average moisture content of the product. The drying kinetics is modeled incorporating a constant rate period followed by a falling rate period. The experimental data obtained using the batch, continuous, single, spiral fluidized bed are matched satisfactorily with the model based on aforementioned assumptions.

The significant parameters of the kinetic model are the drying coefficient during the constant rate period, the initial, critical and the equilibrium moisture contents of the solids. These are affected by the choice of the temperature and the flow rate of the drying medium, the solids holdup and the solids flow rate in continuous operation.

The spiral fluidized dryer, developed in the study, corresponds in its performance to the batch fluidized dryer at high Peclet number and to the single, continuous fluidized dryer at low Peclet number. Axial mixing in spiral fluidized bed is con-

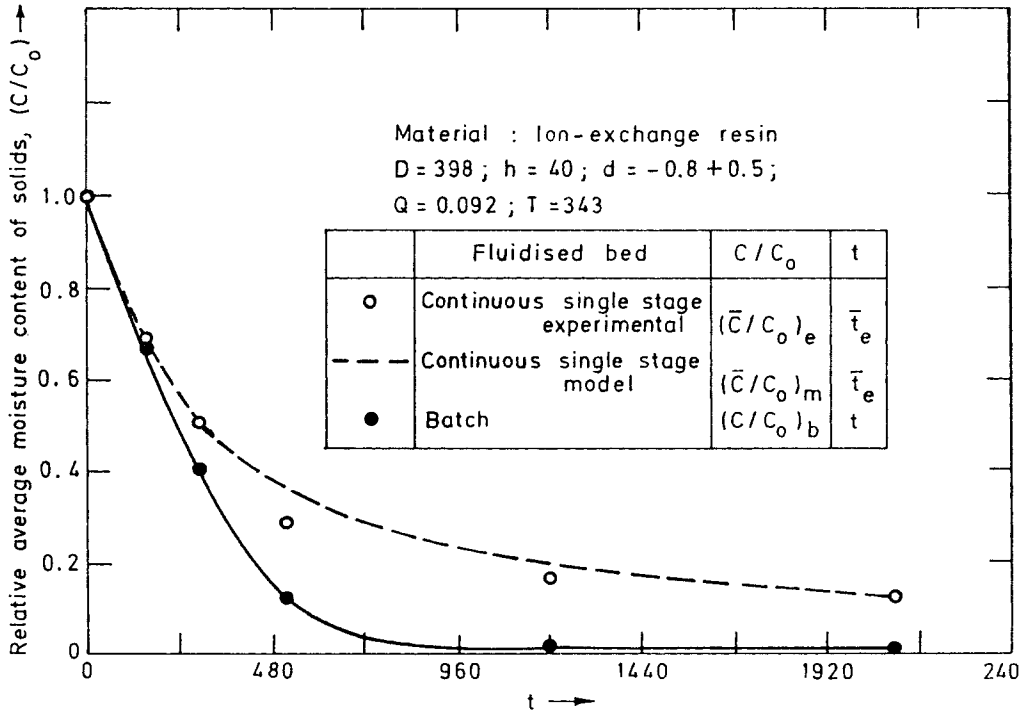

Figure 6. Prediction of the performance of the continuous, single-stage fluidized-bed dryer from batch dryer kinetics.

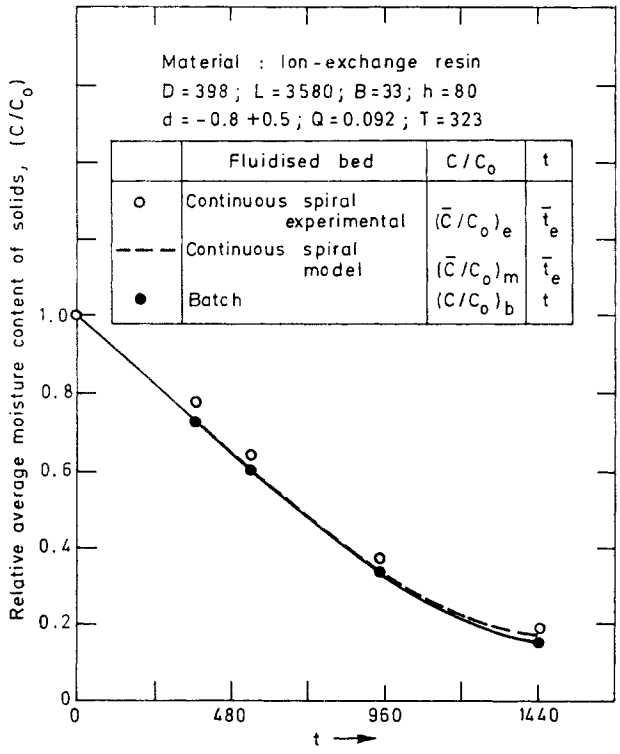

Figure 7. Prediction of the performance of the spiral fluidized dryer from batch dryer kinetics.

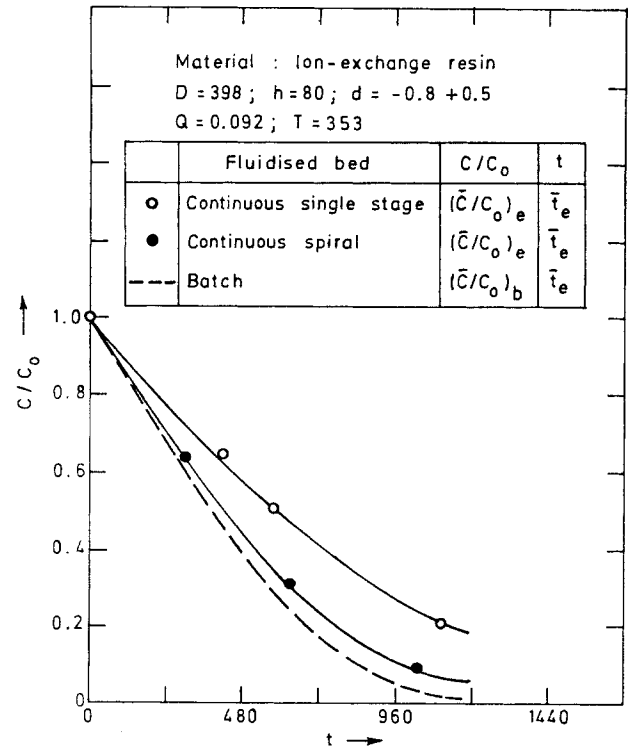

Figure 8. Comparison of the performance of the batch, continuous single-stage and spiral fluidized-bed dryers.

trolled by the choice of the flow rates of the phases and the channel width.

The provision of a spiral in a continuous fluidized dryer enhances its capacity manifold, particularly as the moisture content approaches the equilibrium value in the falling rate period.

Notation

B = channel width, mm
C = moisture content of solid at any time t, kg water/kg dry solid
$\bar{C}$ = average moisture content of the product kg water/kg dry solid
C' = equilibrium moisture content, kg water/kg dry solid
C_c = critical moisture content of solid, kg water/kg dry solid
C_o = initial moisture content of solid, kg water/kg dry solid
$(C/C_o)_b$ = experimentally measured relative moisture content of solid for batch fluidized bed
$(\bar{C}/C_o)_e$ = experimentally measured relative average moisture content of solid for continuous single and spiral fluidized beds
d = effective diameter of the particle, mm
D = diameter of the fluidization column, mm
D_e = dispersion coefficient, cm^2/s
g = acceleration due to gravity, m/s^2
G_s = flow rate of solids, kg/m^2s
h = fluidized bed height, mm
L = length of the channel, mm
Q = volumetric flow rate of the gas, m^3/s
R = constant drying rate, kg water/kg dry solid/s
t = clock time, s
$\bar{t}$ = mean holding time, s
t_c = time corresponding to critical moisture content, s
$\bar{t}_e$ = experimental mean holding time for continuous, single and spiral fluidized beds, s
T = temperature of inlet gas, K
u = superficial velocity of the gas based on column cross-section, m/s
u_s = true average velocity of the solids, m/s
W = holdup of solids, kg

Greek letters

$\beta = R/(C_c - C^*)$, s^{-1}
ϵ = bed porosity
μ = viscosity of gas, kg/m · s
ρ = density of gas, kg/m^3
ρ_s = density of solid, kg/m^3
θ_c = dimensionless time, t/t_c

Dimensionless groups

Ar = Archimedes number, $gd^3\rho(\rho_s - \rho)/\mu^2$
Fr = Froude number, u^2/gd
Pe = Peclet number, u_sL/D_e

Literature Cited

Abramowitz, M., and I. A. Stegun, *Handbook of Mathematical Functions with Formulas, Graphs and Mathematical Tables,* Dover, New York (1972).

Beran, Z., and J. Lutcha, "Optimising Particle Residence Time in a Fluidized Bed Dryer," *The Chem. Engr.*, 678 (1975).

Frolov, V. F., P. G. Romankov, and N. B. Rashkovskaya, "Drying Granular Particles in Multistage Fluidized Bed Apparatus," *Zh. Prikl. Khim,* **37**(4), 824 (1964), cited in *Chem. Abstr.*, **61,** 2747 (1964).

Jobes, C. W., "Fluidized Crystal Dryer Pays Off," *Chem. Eng.*, **61**(1), 166 (1954).

Lykow, A. W., *Experimentalle und Theoretische Grundlagen der Trocknung,* VEB Verlag Technik, Berlin (1955).

Pydisetty, Y., K. Krishnaiah, and Y. B. G. Varma, "Axial Mixing in Spiral Fluidized Beds," *Powder Technol.*, **59,** 1 (1989).

Reay, D., "Particle Residence Time Distributions in Plug-Flow Fluid Bed Dryers," *Proc. Int. Sym. on Drying,* Montreal, Canada, 1 (1978).

Romankov, P. G., "Drying," Chap. 12, *Fluidization*, J. F. Davidson and D. Harrison, eds., Academic Press, London (1971).
Suzuki, K., A. Fujigami, R. Yamazaki, and G. Jimbo, "Some Investigations of Falling Rate Period of Vibro Fluidized-Bed Drying," *J. Chem. Eng. Japan*, **13**(6), 493 (1980).
Vanecek, V., M. Markvart, and R. Drbohlav, *Fluidized bed drying*, Leonard Hill, London (1966).
Vanecek, V., M. Markvart, R. Drbohlav, and R. L. Hummel, "Experimental Evidence on Operation of Continuous Fluidized—bed drier," *Chem. Eng. Prog. Sym. Ser.*, **66**(105), 243 (1970).

Appendix: Continuous, Single Fluidized Dryer

Assuming $E(\theta) = \exp(-\theta)$ for the residence time distribution of solids in continuous, single fluidized dryer, and substituting for (C/C_o) from Eqs. 1 and 2 in dimensionless form, Eq. 3 is written as

$$\frac{\bar{C}}{C_o} = \int_0^{\theta_c}\left(1 - \frac{R\bar{t}\,\theta}{C_o}\right)\exp(-\theta)\,d\theta + \int_{\theta_c}^{\infty}\left[\frac{C^+}{C_o} + \left(\frac{C_c - C^+}{C_o}\right)\exp\{(-\beta\bar{t}(\theta - \theta_c)\}\right]\exp(-\theta)\,d\theta \quad \text{(A1)}$$

Integrating each of the two terms on the righthand side of Eq. A1 by parts and substituting the limits of integration,

$$\int_0^{\theta_c}\left(1 - \frac{R\bar{t}}{C_o}\right)\exp(-\theta)\,d\theta = \left[-\exp(-\theta_c) + \frac{\{\theta_c\exp(-\theta_c) + \exp(-\theta_c)\}R\bar{t}}{C_o} + 1 - \frac{R\bar{t}}{C_o}\right]$$

$$= 1 + \exp(-\theta_c)\left[\frac{R\bar{t}\,\theta_c}{C_o} + \frac{R\bar{t}}{C_o} - 1\right] - \frac{R\bar{t}}{C_o} \quad \text{(A2)}$$

Similarly,

$$\int_{\theta_c}^{\infty}\left[\frac{C^+}{C_o} + \left(\frac{C_c - C^+}{C_o}\right)\exp\{-\beta\bar{t}(\theta - \theta_c)\}\right]\exp(-\theta)\,d\theta = \frac{C}{C_o}\exp(-\theta_c) + \left(\frac{C_c - C^+}{C_o}\right)\frac{\exp(-\theta_c)}{(\beta\bar{t} + 1)} \quad \text{(A3)}$$

Substitution of Eqs. A2 and A3 in Eq. A1 gives Eq. 4. For a system exhibiting only constant rate period, Eq. 4 reduces to

$$\frac{\bar{C}}{C_o} = 1 - \frac{R\bar{t}}{C_o} \quad \text{(A4a)}$$

For a system exhibiting only falling rate period, Eq. 4 reduces to

$$\frac{\bar{C}}{C_o} = 1 - \frac{R\bar{t}}{(\beta\bar{t} + 1)C_o} \quad \text{(A4b)}$$

Spiral fluidized dryer

Substituting for $(C/C_o)_b$ form Eqs. 1 and 2 in dimensionless form and $E(\theta)$ from Eq. 6, Eq. 3 gives:

$$\frac{\bar{C}}{C_o} = \int_0^{\theta_c}\left(1 - \frac{R\bar{t}\,\theta}{C_o}\right)\sqrt{\frac{Pe}{4\pi}}\frac{1}{\theta^{3/2}}\exp\left[-\frac{(1-\theta)^2 Pe}{4\theta}\right]d\theta + \int_{\theta_c}^{\infty}\left\{\frac{C^+}{C_o} + \left(\frac{C_c - C^+}{C_o}\right)\exp[-\beta\bar{t}(\theta - \theta_c)]\right\}$$

$$\cdot\sqrt{\frac{Pe}{4\pi}}\frac{1}{\theta^{3/2}}\exp\left[-\frac{(1-\theta)^2 Pe}{4\theta}\right]d\theta \quad \text{(A4c)}$$

Integrating each of the two terms on the righthand side of Eq. A4c using the principle (Abramowitz and Stegun, 1972)

$$\int\exp\left(-a^2x^2 - \frac{b^2}{x^2}\right)dx = \frac{\sqrt{\pi}}{4a}\left[\exp(2ab)\,\mathrm{erf}\left(ax + \frac{b}{x}\right) + \exp(-2ab)\,\mathrm{erf}\left(ax - \frac{b}{x}\right)\right] + \text{constant}, \quad a \neq 0 \quad \text{(A4d)}$$

we obtain,

$$\frac{\bar{C}}{C_o} = \frac{1}{2}\exp\left(\frac{Pe}{2}\right)\left[\exp\left(\frac{Pe}{2}\right)\left(1 + \frac{R\bar{t}}{C_o} - \frac{C^+}{C_o}\right)\cdot\left\{1 - \mathrm{erf}\left(\sqrt{\frac{Pe}{4\theta_c}} + \sqrt{\frac{Pe\theta_c}{4}}\right)\right\} - \exp\left(-\frac{Pe}{2}\right)\left(1 - \frac{R\bar{t}}{C_o} - \frac{C^+}{C_o}\right)\cdot\mathrm{erf}\left(\sqrt{\frac{Pe}{4\theta_c}} - \sqrt{\frac{Pe\theta_c}{4}}\right) + \left(\frac{C_c - C^+}{C_o}\right)\exp(\beta\bar{t}\,\theta_c)\cdot\left\{\exp\left(\sqrt{Pe}\sqrt{\frac{Pe}{4} + \beta\bar{t}}\right)\left[\mathrm{erf}\left(\sqrt{\frac{Pe}{4\theta_c}} + \sqrt{\left(\frac{Pe}{4} + \beta\bar{t}\right)\theta_c}\right) - 1\right] + \exp\left(-\sqrt{Pe}\sqrt{\frac{Pe}{4} + \beta\bar{t}}\right)\cdot\left[\mathrm{erf}\left(\sqrt{\frac{Pe}{4\theta_c}} - \sqrt{\left(\frac{Pe}{4} + \beta\bar{t}\right)\theta_c}\right) + 1\right]\right\} + \frac{1}{2}\left(1 - \frac{R\bar{t}}{C_o} + \frac{C^+}{C_o}\right) \quad \text{(A4e)}$$

Substituting

$$\beta = \frac{R}{C_c - C^+}$$

and

$$1 - \frac{C^+}{C_o} = \frac{1}{C_o}\left[Rt_c + \frac{R}{\beta}\right]$$

Equation A4e is simplified to give Eq. 7. For a system exhibiting only constant rate period, Eq. 7 reduces to Eq. A4a. For a system exhibiting only falling rate period, Eq. 7 reduces to

$$\frac{\bar{C}}{C_o} = \frac{C^+}{C_o} + \left(\frac{C_o - C^+}{C_o}\right)\exp\left[\frac{Pe}{2} - \sqrt{Pe\left(\frac{Pe}{4} + \beta\bar{t}\right)}\right] \quad \text{(A7a)}$$

Manuscript received Mar. 13, 1989, and revision received Sept. 12, 1989.